

Fabrication of microresonators by using photoresist developer as etchant

Shu-Qing Song(宋树清), Jian-Wen Xu(徐建文), Zhi-Kun Han(韩志坤), Xiao-Pei Yang(杨晓沛), Yu-Ting Sun(孙宇霆), Xiao-Han Wang(王晓晗), Shao-Xiong Li(李邵雄), Dong Lan(兰栋), Jie Zhao(赵杰), Xin-Sheng Tan(谭新生), and Yang Yu(于扬)

Citation: Chin. Phys. B, 2021, 30 (**6**): 060313. DOI: 10.1088/1674-1056/abf112
Journal homepage: http://cpb.iphy.ac.cn; http://iopscience.iop.org/cpb

What follows is a list of articles you may be interested in

Nb-based Josephson parametric amplifier for superconducting qubit measurement

Fei-Fan Su(宿非凡), Zi-Ting Wang(王子婷), Hui-Kai Xu(徐晖凯), Shou-Kuan Zhao(赵寿宽), Hai-Sheng Yan(严海生), Zhao-Hua Yang(杨钊华), Ye Tian(田野), Shi-Ping Zhao(赵士平)

Chin. Phys. B, 2019, 28 (**11**): 110303. DOI: 10.1088/1674-1056/ab4578

Solid-state quantum computation station

Fanming Qu(屈凡明), Zhongqing Ji(姬忠庆), Ye Tian(田野), Shiping Zhao(赵士平)

Chin. Phys. B, 2018, 27 (**7**): 070301. DOI: 10.1088/1674-1056/27/7/070301

Invariants-based shortcuts for fast generating Greenberger—Horne—Zeilinger state among three superconducting qubits

Jing Xu(徐晶), Lin Yu(于琳), Jin-Lei Wu(吴金雷), Xin Ji(计新)

Chin. Phys. B, 2017, 26 (**9**): 090301. DOI: 10.1088/1674-1056/26/9/090301

Fast generating *W* state of three superconducting qubits via Lewis-Riesenfeld invariants

Lin Yu(于琳), Jing Xu(徐晶), Jin-Lei Wu(吴金雷), Xin Ji(计新)

Chin. Phys. B, 2017, 26 (**6**): 060306. DOI: 10.1088/1674-1056/26/6/060306

Creating nitrogen–vacancy ensembles in diamond for coupling with flux qubit

Ya-Rui Zheng(郑亚锐), Jian Xing(邢健), Yan-Chun Chang(常彦春), Zhi-Guang Yan(闫智广), Hui Deng(邓辉), Yu-Lin Wu(吴玉林), Li Lü(吕力), Xin-Yu Pan(潘新宇), Xiao-Bo Zhu(朱晓波), Dong-Ning Zheng(郑东宁)

Chin. Phys. B, 2017, 26 (**2**): 020305. DOI: 10.1088/1674-1056/26/2/020305

SPECIAL TOPIC — Quantum computation and quantum simulation

Fabrication of microresonators by using photoresist developer as etchant*

Shu-Qing Song(宋树清), Jian-Wen Xu(徐建文), Zhi-Kun Han(韩志坤), Xiao-Pei Yang(杨晓沛), Yu-Ting Sun(孙宇霆), Xiao-Han Wang(王晓晗), Shao-Xiong Li(李邵雄), Dong Lan(兰栋), Jie Zhao(赵杰), Xin-Sheng Tan(谭新生), and Yang Yu(于扬)†

National Laboratory of Solid State Microstructures, School of Physics, Nanjing University, Nanjing 210093, *China*

(Received 18 November 2020; revised manuscript received 2 March 2021; accepted manuscript online 23 March 2021)

In superconducting circuit, microwave resonators and capacitors are crucial components, and their quality has a strong impact on circuit performance. Here we develop a novel wet etching process to define these two components using common photoresist developer as etchant. This method reduces subsequent steps and can be completed immediately after development. By measuring the internal quality factor of resonators, we show that it is possible to achieve similar or better performance when compared with samples made by standard etching processes. This easy-to-implement method may boost the yield hence providing an alternative fabrication process for microwave resonators and capacitors.

Keywords: superconducting qubit, microresonator, easy-to-implement, high quality factors

PACS: 03.67.Lx, 85.25.Am **DOI:** 10.1088/1674-1056/abf112

1. Introduction

Through two decades development, the superconducting transmon qubit system has enable demonstrations of quantum supremacy,[1,2] quantum algorithms,[3–6] quantum error correction,[7–9] and quantum chemical simulation.[10,11] Nevertheless, in order to realize fault tolerant quantum computing, people pursue longer decoherence time for implementing more high fidelity gate operations before significant error ruins the information. An important source of decoherence is the energy ralaxation. Great efforts have been made to improve the relaxtion time T_1.[12–15] In general, superconducting quantum circuits consist not only the Josephson junctions as the key parts to supply the nonlinearity and constitute the artificial atom, but also microwave resonators to protect and readout the qubit. Additionally, capacitors are usually used to minimize the charge dispersion.[16] Recent investigations show that T_1 can be limited by possible imperfections in the Josephson junctions and microwave dielectric losses.[17–21] In general process, superconducting 2D transmon qubits are fabricated by depositing aluminum film on high-purity sapphire substrate. Aluminum has a dense oxidation layer and a reasonable superconducting transition temperature, while sapphire has a low loss tangent less than 10^{-9}.[22] Due to the coupling of the qubits and microwave resonator, it is usual that the the upper limit of T_1 is set by the resonator internal quality factor Q_i, i.e., $T_1 < Q_i/\omega_{10}$, where ω_{10} is the qubit angular frequency, and $\hbar\omega_{10}$ is the energy difference of qubit states. Therefore, a high quality microwave resonator is indispensable for a high performance qubit system. During the fabrication, the resonators are defined by lithography and etch. These processes produce defects which form the two-level systems (TLS).[23,24] The loss resulting from the coupling between the qubits and TLS is thought to be the dominate source of the energy relaxation. It is known that TLS loss is generated mainly in bulk dielectrics and at the interfaces between materials.[25]

Traditionally, resonators are fabricated by either dry etching or wet chemical etching. Dry etching with chlorine and boron trichloride is considered as a very efficient method. However, the photoresist is hard to remove after reacting with chlorine ions. The residue resist will cause energy loss. Subsequent treatments have to be applied and complicated the fabrication process, resulting a dramatic decrease of the yield of a perfect chip. On the other hand, traditional wet chmical etching brings extra acidic ions that add more uncertainty to the system. Exploring new etching technique is helpful for fabricating high quality superconducting quantum circuits.

Here we develop a novel wet chemical etch process to define the microwave resonators and capacitors using photoresist developer ZJX-238 (tetramethyl ammonium hydroxide) instead of traditional wet etch chemicals with aluminum etch type A. Moreover, etch can be done with developer immediately after development. We use a standard Xmon design[26] to compare the three processes with the same treated sapphire substrate and aluminum film. The quality factors of resonators from three different processes are measured in a dilution re-

*Project supported by the National Key R&D Program of China (Grant No. 2016YFA0301802), the National Natural Science Foundation of China (Grant Nos. 61521001 and 11890704), and the Key R&D Program of Guangdong Province, China (Grant No. 2018B030326001).

†Corresponding author. E-mail: yuyang@nju.edu.cn

© 2021 Chinese Physical Society and IOP Publishing Ltd

frigerator. The results indicate that the resonators etched by ZJX-238 perform similar or better than that fabricated by the other two processes. It provides an alternative method of fabricating high quality microwave resonators for superconducting qubits.

2. Fabrication and experiment

The resonators are fabricated on *c*-plane sapphire substrate (Roditi) that are 0.43 mm thick and single-side polished. The wafer is cleaned with UV ozone cleaner immediately before loading into the electron beam evaporation. Then 100 nm aluminum is deposited on the sapphire substrate at high vacuum environment (approximately 10^{-9} mbar).

Details of the process to form the microwave resonators are illustrated in Fig. 1. Due to the size and resolution of the coplanar waveguide cavity, we use a standard S1805 resist (≈500 nm thickness). As shown in Fig. 1(a), the resist is patterned using a direct-write process which has 5 mm write head on Heidelberg DWL 66+ laser writer. After developing 30 s in ZJX-238 developer (Fig. 1(b)), the resist is hard-baked for 2 min at 115 °C. Next, the aluminum is etched in ZJX-238 for about 4 min at room temperature (Fig. 1(c)). Figure 1(d) shows a complete coplanar waveguide resonator after stripping resist, then the chips are diced into 10 mm × 10 mm squares. At last the completed devices are packaged into a sample holder and measured in a dilution refrigerator which has a base temperature about 20 mK.

Figures 2(a) and 2(b) show the images of our device and schematic of our measurement setup. The ten $\lambda/4$ coplanar waveguide resonators ($\omega_R/2\pi$ ranging from 6.62–6.87 GHz) are inductively coupled to readout transmission line. Attenuators and low-pass filters are installed in the microwave input

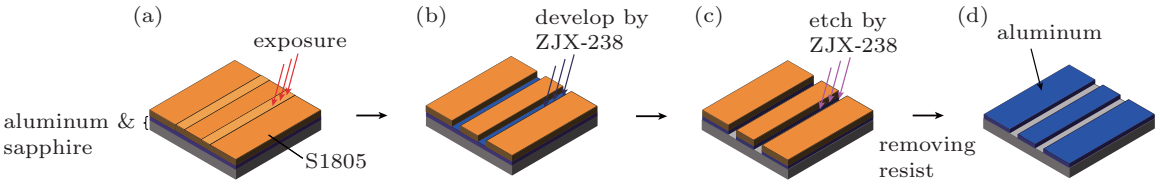


Fig. 1. Fabrication process flow of the resonators. (a) 3D view of the device exposed by direct laser writing after evaporation of Al with photoresist. (b) Form a pattern of resonators while the exposed resist is removed by developer (ZJX-238). (c) Etching by ZJX-238 immediately defines the electrode of the chip. (d) Complete resonators after the resist-removing process.

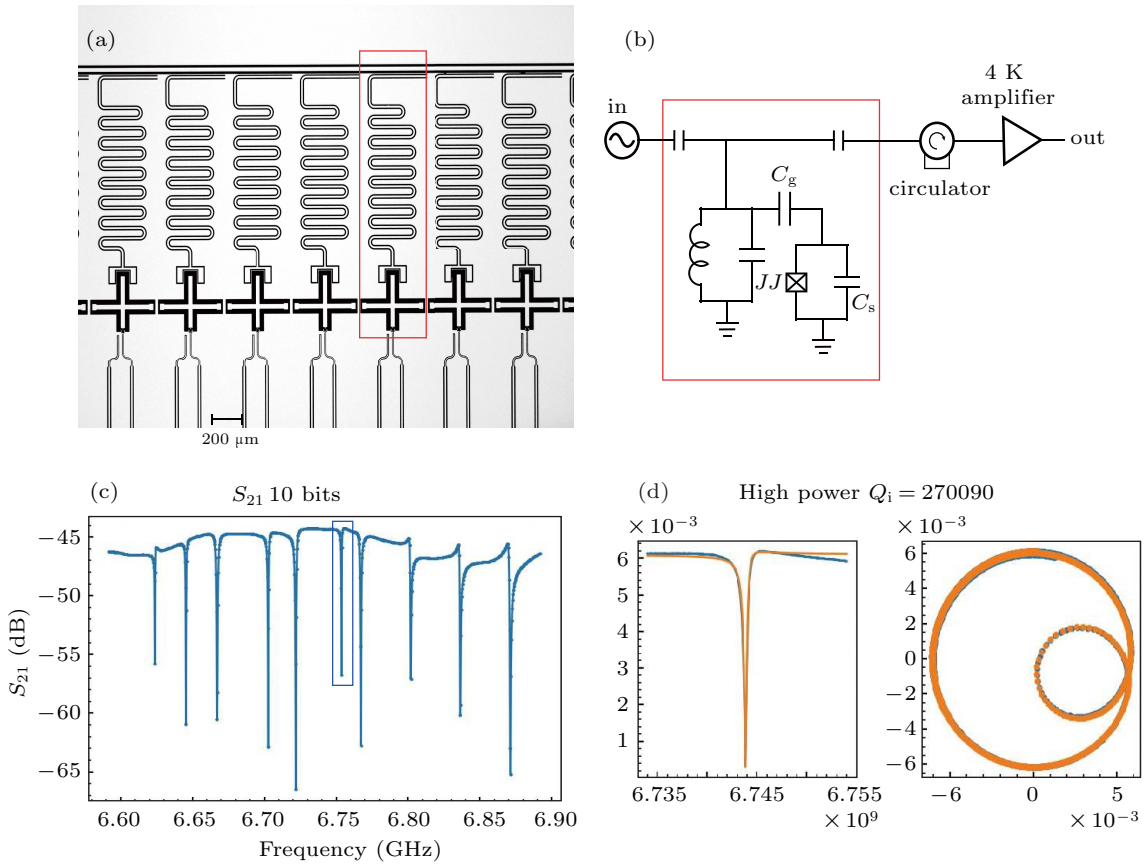


Fig. 2. Micrographs and measurement of the resonators. (a) Optical images of our ten transmon qubits device, the resonator is realized in microstrip geometry with a measured frequency $\omega_R/2\pi$ range from 6.62–6.87 GHz. (b) Circuit schematic of the red frame above. (c) S_{21} of the ten resonators measured by network analyzer. (d) Q_i of the resonator in the blue frame is fitted to be about 270000 at high power.

line to prevent leakage of thermal radiation into the resonator. The signal, after passing the sample, is amplified by a cryogenic high-electron mobility transistor (HEMT) and room-temperature amplifier.

As shown in Fig. 2(c), we measured the magnitude and phase of the transmitted signal S_{21} using a network analyzer to extract the quality factors. Normally, an asymmetry in the coupling of a resonator to the input and output ports results in deviation of the resonator response from a symmetric Lorentzian function.[27] Note the slight asymmetry about the resonators, which can be attributed to a small impedance mismatch in the central transmission line on either side of the resonator, likely originated from the sample imperfections, wirebond connections, or the transmission line geometry.[28] Quality factor of the resonator is fitted by the following equation at resonance frequency:

$$\tilde{S}_{21}^{-1} = 1 + \frac{Q_\mathrm{i}}{Q_\mathrm{c}^*} \mathrm{e}^{\mathrm{i}\phi}. \tag{1}$$

A normalized inverse transmission $\tilde{S}_{21}^{-1}$ is defined with Q_i and Q_c^*, which are the internal and rescaled coupling quality factors, respectively. In this representation, the resonator response is a circle starting and ending at $\tilde{S}_{21}^{-1} = 1$ and the circle center is rotated from the real axis by the impedance mismatch angle ϕ. Figure 2(d) shows the Q_i of the resonator in blue frame that has been fitted.

3. Characterizations and results

We spray a thin layer of gold to improve the contrast between aluminum and sapphire and show scanning electron microscopes (SEM) images of the fabricated coplanar waveguide resonator in Fig. 3(a) from 45° above the slop. It is clear that there is no visible contaminant at the micron scale. Atomic force microscope (AFM) images in Fig. 3(b) as the supplement of SEM enable us to characterize the interface. The graph at right depicts the morphology of the interface and the altitude variation along the horizontal axis. The left panel shows the 1D plot along the white dotted line.

The inverse of resonator Q_i is represented as the loss tangent

$$1/Q_\mathrm{i} = \tan\delta \simeq \delta. \tag{2}$$

Loss is a convenient metric for distinguishing between multiple contributions to performance while Q_i is used to compare general performance, especially for high performance devices. Etching brings loss thought to be dominated by coupling to two-level systems (TLS). Therefore, the interface between the superconductor and the substrate may be the largest source of TLS loss. According to the TLS model,[29] the resonator loss δ_TLS at low constant temperature follows the empirical formula

$$\delta_\mathrm{TLS} \propto (N + P_\mathrm{input})^{-\frac{1}{2}}, \tag{3}$$

where P_input is the actual input power to the resonator that can be calculated by the power input from the network analyzer minus the attenuation on the line, N is a constant related to the characteristic photon number of TLS saturation. With the input power increasing, the δ_TLS decreases and the impact of TLS on the system is reduced. Therefore, we can measure the effect of TLS contributing to the system by comparing the internal quality factors between low power and high power.

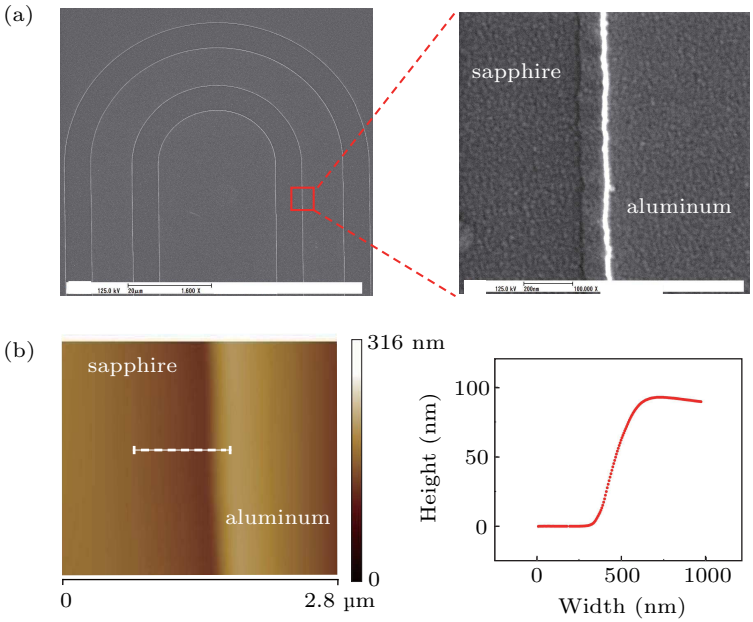


Fig. 3. Characterization of the etched interface. (a) SEM images of our coplanar waveguide resonator from 45° above the slope. The figure on the right is magnified 100000 times and it shows smooth interface between sapphire and aluminum. (b) AFM images in the same place, colorbar indicates the relative altitude. The graph at right shows the altitude variation along the horizontal axis. The left panel shows the 1D height change along the white dotted line.

As shown in Fig. 4(a), we compare the quality factor gaps of high power and low power in ten resonators. The result indicates that there is a little TLS formed in the system during etching. To figure out whether this new process could be a substitute for dry etching or wet etching by aluminum etch type A, we make a comparison with the three processes by controlling variables with the same treated sapphire substrate and aluminum film evaporated by electron beam to fabricate 10 resonators. As shown in Fig. 4(b), the internal quality factors of resonators etched by ZJX-238 are similar or even better than the other two. Considering that our novel wet etch omits the subsequent process, it is more convenient during the fabrication. The decrease of the time and complexity of fabrication will increase the yielding of the superconducting circuits.

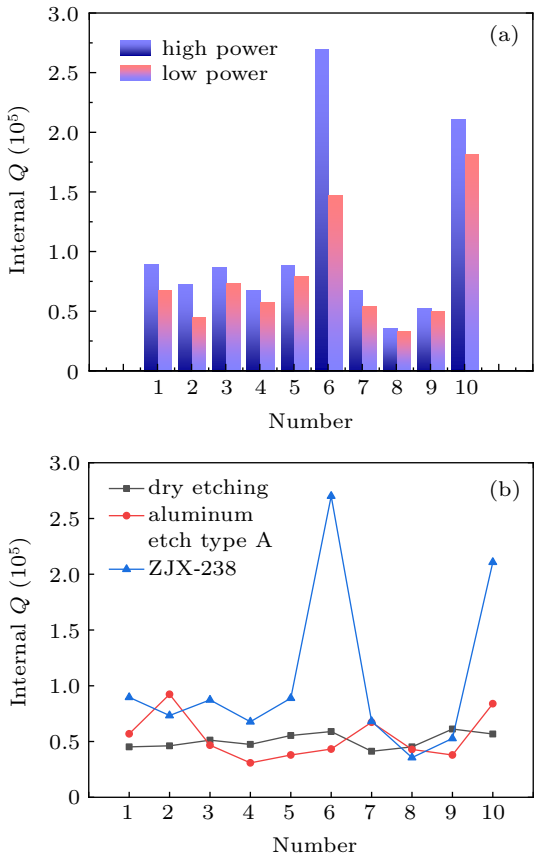


Fig. 4. Internal quality factor comparison. (a) High power quality factor versus low power of the ten resonators etched with ZJX-238. (b) Comparison of ten resonators of three different etching processes with quality factors variation, indicating that resonators etched by ZJX-238 have an advantage over the other two.

4. Summary

In conclusion, we presented an alternative method of fabricating microwave resonators and capacitors for superconducting qubits. This method only involves development process after lithography and etching with the same solution, which makes it compatible with a large scale fabrication process. We also demonstrated that a 2D transmon qubit made with ZJX-238 still has a high quality and higher yield. It provides an alternative fabrication process for microwave resonators and capacitors.

References

[1] Arute F, Arya K, Babbush R, *et al.* 2019 *Nature* **574** 7779
[2] Jurcevic P, Javadi-Abhari A, Bishop L S, *et al.* 2021 *Quantum Science and Technology* **6** 025020
[3] Montanaro A 2016 *npj Quantum Information* **2** 1
[4] O'Malley P J J, Babbush R, Kivlichan I D, *et al.* 2014 *Phys. Rev.X* **6** 031007
[5] Pei P, Huang H F, Guo Y Q, Song H S2016 *Chin. Phys. Lett.* **33** 020301
[6] Zhao J, Hu Y Y, Tong P Q2015 *Chin. Phys. Lett.* **32** 060501
[7] Ofek N, Petrenko A, Heeres R, *et al.* 2016 *Nature* **536** 7617
[8] Reed M D, DiCarlo L, Nigg S E, *et al.* 2012 *Nature* **482**7385
[9] Havlíček V, Córcoles A D, Temme K, *et al.* 2019 *Nature* **567** 7747
[10] Google AI Quantum 2020 *Science* **369** 6507
[11] Hempel C, Maier C, Romero J, *et al.* 2018 *Phys. Rev. X* **8** 031022
[12] Kjaergaard M, Schwartz M E, Braumüller J, *et al.* 2020 *Annual Rev. Condensed Matter Phys.* **11** 369
[13] Stehli A, Brehm J D, Wolz T, *et al.* 2020 *Appl. Phys. Lett.* **117** 124005
[14] Place A P M, Rodgers L V H, Mundada P, *et al.* 2020 arXiv: 2003.00024
[15] Nersisyan A, Poletto S, Alidoust N, *et al.* 2019 *IEEE International Electron Devices Meeting (IEDM)* 31.1.1–31.1.4
[16] Koch J, Terri M Y, Gambetta J, *et al.* 2007 *Phys. Rev. A* **76** 042319
[17] Kamal A, Yoder J L, Yan F, *et al.* 2016 arXiv:1606.09262
[18] Wang C, Axline C, Gao Y Y, *et al.* 2015 *Appl. Phys. Lett.* **107** 162601
[19] Serniak K, Hays M, De Lange G, *et al.* 2018 *Phys. Rev. Lett.* **121** 157701
[20] Wang C, Gao Y Y, Pop I M, *et al.* 2014 *Nat. Commun.* **5** 1
[21] Gustavsson S, Yan F, Catelani G, *et al.* 2016 *Science* **354** 6319
[22] Braginsky V B, Ilchenko V S, Bagdassarov K S 1987 *Phys. Lett. A* **120** 6
[23] Melville A, Calusine G, Woods W, *et al.* 2020 *Appl. Phys. Lett.* **117** 124004
[24] Wang Y Y, Fang M F 2020 *Chin. Phys. B* **29** 030304
[25] Martinis J M, Cooper K B, McDermott R, *et al.* 2016 *Phys. Rev. Lett.* **95** 210503
[26] Barends R, Kelly J, Megrant A, *et al.* 2013 *Phys. Rev. Lett.* **111** 080502
[27] Khalil M S, Stoutimore M J A, Wellstood F C, *et al.* 2012 *J. Appl. Phys.* **111** 054510
[28] Megrant A, Neill C, Barends R, *et al.* 2012 *Appl. Phys. Lett.* **100**113510
[29] Phillips W A 1987 *Reports on Progress in Physics* **50** 1657